Nanoscale ripples on polymers created by a focused ion beam

Myoung-Woon Moon[1]**, Jun Hyun Han**[2]**, Ashkan Vaziri**[3,6]**,
Eun Kyu Her**[4]**, Kyu Hwan Oh**[4]**, Kwang-Ryeol Lee**[1] **and
John W Hutchinson**[5,6]

[1] Future Fusion Technology Laboratory, Korea Institute of Science and Technology,
Seoul 136-791, Republic of Korea
[2] Materials Science and Technology Research Division, Korea Institute of Science and
Technology, Seoul 136-791, Republic of Korea
[3] Department of Mechanical and Industrial Engineering, Northeastern University, Boston,
MA 02115, USA
[4] Department of Materials Science and Engineering, Seoul National University,
Seoul 151-744, Republic of Korea
[5] School of Engineering and Applied Sciences, Harvard University, Cambridge,
MA 02138, USA

E-mail: vaziri@coe.neu.edu and jhutchin@fas.harvard.edu

Abstract
We show that focused ion beam irradiation results in the creation of peculiar one- and
two-dimensional nanoscale features on the surface of polyimide—a common polymer in
electronics, large scale structures, and the automobile industry, as well as in biomedical
applications. The role of ion beam incident angle, acceleration voltage, and fluence on the
morphology of the structural features is systematically investigated, and insights into the
mechanisms of formation of these nanoscale features are provided. Moreover, by using the
maskless patterning method of the focused ion beam system, we have developed a robust
technique for controlled modification of the polymeric surface. The technique, which is
analogous to using a gray glass with varying darkness to control the radiation from the sun, but
at a much smaller scale, enables the ion intensity and angle to be controlled at each surface point
of the polymer, giving rise to structural surface features with desired shape and morphology.

M This article features online multimedia enhancements

(Some figures in this article are in colour only in the electronic version)

1. Introduction

Ion beam irradiation has been used extensively for surface
modification of polymers, glassy metals, and amorphous and
crystalline materials at micron and submicron scales [1–6].
The surface structures created by exposure to an ion beam
range from dots, steps, and one-dimensional (1D) straight
wrinkles to highly complex hierarchical undulations and
ripples [5–13]. In general, the morphology of these nanoscale
features can be selected by controlling the ion beam parameters
(e.g. fluence and acceleration voltage), making ion beam

irradiation a promising method for the surface engineering
of materials. An example is the recent experiments on
polydimethalsiloxane (PDMS) [13–15], which have provided
new avenues for controlled surface modification. The
irradiation of a Ga^+ focused ion beam (FIB) on the surface of
a compliant polymer results in the formation of a wrinkled stiff
skin on the polymer, with overall morphology and wavelength
that can be controlled by selecting the ion beam parameters.
The capabilities of this technique have been recently extended
by using maskless patterning of the focused ion beam
system [13–15]. This yields a robust technique for controlled
surface modification that can be used for a wide range of

[6] Authors to whom any correspondence should be addressed.

interdisciplinary applications including microfluidics, flexible electronics, biosensors, tissue engineering, and regenerative medicine [16–18].

In this paper, we examine for the first time the effect of focused ion beam irradiation on a polyimide (PI) substrate—a much stiffer polymer than PDMS, with an elastic modulus of 1–10 GPa (compared to ~1 MPa for PDMS [19]). Polyimide, due to its unique properties (e.g. high strength, and heat and chemical resistance) as well as its excellent biostability and biocompatibility properties, has become a very common polymer in electronics, large scale structures, and the car industry, as well as in biomedical applications [20–25]. We show that ion beam irradiation leads to the formation of ripples on the PI surface, with morphology and direction that can be controlled by the ion beam parameters. We provide some insights into the mechanisms of formation of these peculiar structural features by examining the chemical compositions of the polymer surface after irradiation.

In a second set of experiments, we have developed a robust technique for the creation of structural features on selected small surfaces of the polymer using the maskless patterning method of a focused ion beam system. Examples of the peculiar three-dimensional (3D) features created on the PI surface using the technique are provided. The key advantages and some of the potential applications of the proposed technique are also highlighted briefly.

2. Experimental details

Polyimide (UPILEX-25S, JAPAN) coupons of size 20 mm × 20 mm × 0.1 mm were used in our experiment with an elastic modulus ~ 9 GPa and density 1.47 g cm^{-3} (at room temperature). A field emission (FE)-SEM/FIB dual beam system (FE-SEM/FIB Dual Beam NOVA; FEI, Hillsboro, OR) was used for focused ion beam irradiation. The polyimide coupons were placed in the high vacuum chamber under a working pressure of ≈10^{-5} Pa. Prior to ion beam exposure, a 3 nm Au layer was deposited on the polyimide substrate to prevent the polymer surface from electron-charging.

The acceleration voltage and ion current were varied over the ranges 10–30 keV and 1–20 nA, respectively. The irradiation angle, defined as the angle between the incoming beam and the surface normal, was varied between 0° and ~90°. The beam dwell time was kept at 3 μs in all the experiments. The images in the exposed region were taken with a built-in secondary electron microscope (SEM) in the FE-SEM/FIB system. The morphology of the surface structures was examined using an atomic force microscope (AFM; Nanoscope III, Digital Instrument, NY) in the tapping mode at ambient conditions. In each experiment, the morphology of the surface patterns was typically measured on five different surface regions of the polymer.

The cross-sectional microstructure (prepared with the FE-SEM/FIB system) of the polymeric substrate near its surfaces was explored with a high-resolution transmission electron microscope (TEM; JEM-3000F, JEOL). Moreover, the chemical composition of the surface layer through the depth was analyzed using energy dispersive x-ray spectroscopy (EDS, OXFORD). Electron energy loss spectroscopy (EELS), in conjunction with a high voltage electron microscope (HVEM, JEOL), was also employed to examine the compositional change of the surface layer on the PI surface induced by FIB irradiation.

The maskless patterning method of the FIB equipment was adopted for the creation of 3D morphologies guided by predefined bitmap images. This method permits the accurate selection of the areas exposed to the FIB. Bitmap files of the exposure patterns were imported as a virtual mask in the FIB system. Then, the surface area of the PI substrate (20 μm × 20 μm) was subjected to the FIB irradiation.

3. Results and discussion

Figure 1(A) shows the schematics of the experiment, in which a 10 μm × 10 μm surface area of the PI substrate was subjected to the ion beam at a constant incident angle and acceleration voltage. When the incident angle is normal to the surface, the exposure of the surface to the ion beam results in milling of the substrate with no surface undulation and instability. A similar set of experiments was performed on a Si substrate, leading to a similar outcome. The dependence of the milling depth on the fluence and acceleration voltage of the ion beam is quantified for both PI and the Si substrate in figure 1(B). Here, the milling depth was measured by the SEM as the exposure time increased from 30 to 600 s (corresponding to an ion fluence of 4.6×10^{16} to 47×10^{16} ions cm^{-2}) at two ion acceleration voltages. Interestingly, the milling rate is very similar for both PI and the Si substrate. Figures 1(C) shows the patterns created by the FIB irradiation on the PI surface at incident angles of 45° and 85°, and the evolution of the patterns as the exposure time and, therefore, ion fluence, increases. The ion beam irradiation leads to the creation of nanoscale structural features on the polymeric surface, which manifest themselves as nanoscale ripple morphologies. For the ion incident angle 45°, the ripple vector was first created parallel to the projected ion beam (black arrow). With increasing exposure time, the amplitude of the ripples increases, while the wavelength of the ripples is almost constant, at 320 nm. For an ion beam incident angle 85°, the ripple structures appear as 1D undulations but normal to the projected ion beam. Now with increased exposure time, the 1D ripple morphology evolves to complex 1D columnar patterns, while the amplitude of the patterns increases rapidly. The wavelength of the ripples increases slightly with the exposure duration from ~300 to ~500 nm for 30 keV. The acceleration voltage and current of the ion beam in this set of experiments were 30 keV and 7 nA, respectively. The dependence of the amplitude and wavelength of the morphologies will be taken up again in what follows.

To further explore the role of the ion beam incident angle on the morphology of the patterns created by the focused ion beam, we systematically varied the incident angle between 0° (normal to the surface) and 85° (almost parallel to the surface) by keeping the acceleration voltage and current of the ion beam as 30 keV and 7 nA, respectively—see figure 2(A). As noted earlier, ion beam irradiation at an incident angle close to the surface normal leads to surface milling with no
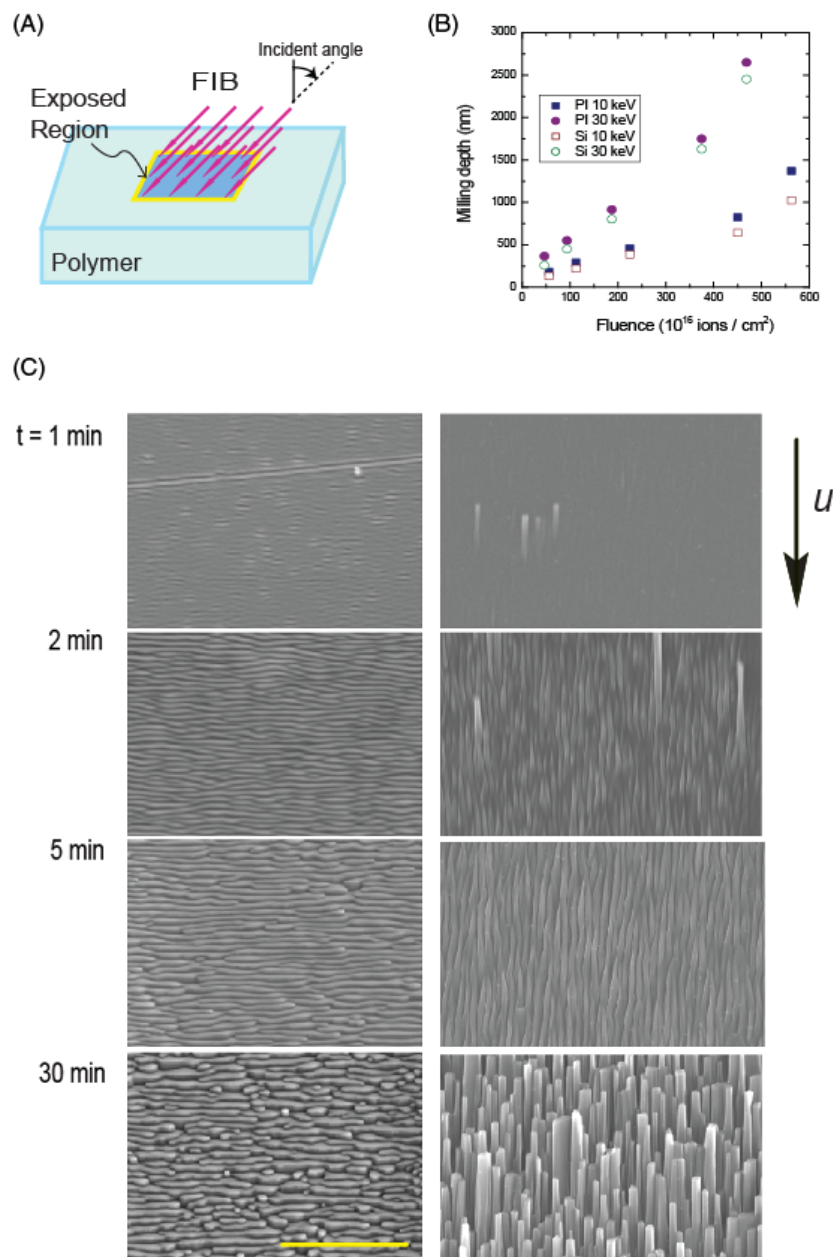
Figure 1. Creation of ripples on the surface of polyimide by a focused ion beam. (A) Schematic of the experiment. (B) Milling depth versus ion fluence for both PI and SI substrate subject to focused ion beam irradiation with incident angle 0° at two acceleration voltages, 10 and 30 keV. (C) Evolution of the polyimide surface by exposure to ion beam at the incident angle (projection direction of ion beam, *u*) of 45° (left panels) and 85° (right panels). The acceleration voltage and ion current were 30 keV and 7 nA, respectively, for this set of experiments. Scale bar = 5 *μ*m.

surface undulation and instability—as quantified in figure 1(B). With increasing incident angle, ripple morphologies appear at a critical angle of approximately 30° for this set of ion beam parameters. This is confirmed by examining the surface using an atomic force microscope in the tapping mode at ambient conditions. The ripple patterns on the polymeric surface created at the incident angle 30° have the wavevector aligned along the ion beam projected direction. With further increase in the incident angle, the formation of two-dimensional (2D) columnar structures sets in, at the incident angle ∼55°. This critical incident angle is found not to be very sensitive to the

ion accelerating voltage in the range studied here (5–30 keV). A further increase in the incident angle (>80°, where the ion beam is approximately parallel to the polymer surface) leads to the formation of 1D ripple morphologies but normal to the direction of irradiation. The underlying mechanisms producing these peculiar morphologies and their transitions tied to the incident beam angle are not understood. It is noteworthy that the peculiar transition in surface structure with change in the incident angle has been also observed in experiments on aluminum thin films [26] and Si/amorphous Si [8, 9]. It was suggested that once a ripple pattern forms by ion beam
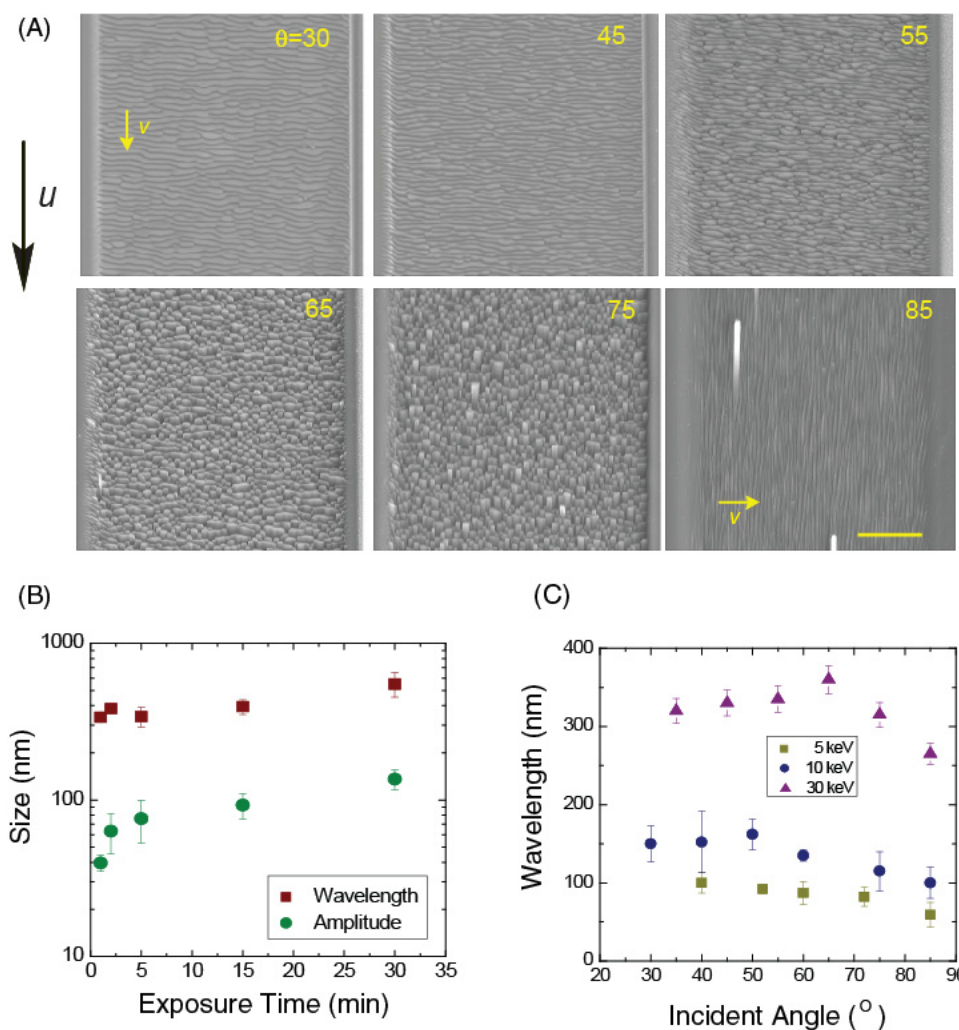
Figure 2. Ordered structural features created at different ion beam incident angles (θ). (A) The panels show the morphology of the patterns created on the surface of originally flat polyimide substrate by 3 min exposure to the focused ion beam along the projection direction *u*. The acceleration voltage and current density of the ion beam were 30 keV and 7 nA, respectively. Scale bar $= 5$ μm. (B) Amplitude and wavelength of ripple structures created by focused ion beam irradiation with incident angle 50°, versus the exposure time. The acceleration voltage and current density of the ion beam were 30 keV and 7 nA, respectively. (C) Role of ion beam incident angle on the wavelength of created ordered structures for three acceleration voltages (5, 10, and 30 keV) at 5 min exposure time. The current density of the ion beam was 7 nA.

irradiation, the erosion rate at the valley regions (concave region) of ripple patterns can be higher than that at the convex region [1], which could lead to this transition from the step-like structure into 1D-like surface structures with increase of ion fluence or exposure time.

Figures 2(B) and (C) show the role of ion beam parameters on the morphology of the patterns. The wavelength and amplitude of patterns created at different acceleration voltage, incident angle, and ion fluence were measured using an AFM. The wavelength of the patterns is mainly controlled by the ion beam acceleration voltage, while the amplitude is mainly dependent on the fluence or, equivalently, on the irradiation time (see figure 2(B) for a set of results measured at the ion incident angle 50° and acceleration voltage 30 keV). The wavelength increases only slightly with the exposure time (in the range 300–500 nm), while the amplitude is much more sensitive to this parameter. Figure 2(C) shows the dependence

of the wavelength and amplitude of the structural features on the ion beam incident angle for three acceleration voltages: 5, 10, and 30 keV. The wavelengths of the patterns increased from ∼55 to ∼370 nm, while slightly depending on the incident angle.

To explore the mechanisms of formation of surface features, we examined the chemical composition of the surface layer through the depth. Figure 3(A) shows the cross section of the polymeric substrate at the region exposed to the ion beam with incident angle 55°. For this beam incident angle, the induced ripple patterns have the wavevector aligned along the ion beam projected direction. The figure shows anisotropic undulation with respect to the ion beam orientation. TEM analysis was performed to examine the chemical composition of the exposed region of the PI substrate with depth. We examined the polyimide surface exposed to the ion beam along depth using high resolution TEM (HRTEM) analysis. The
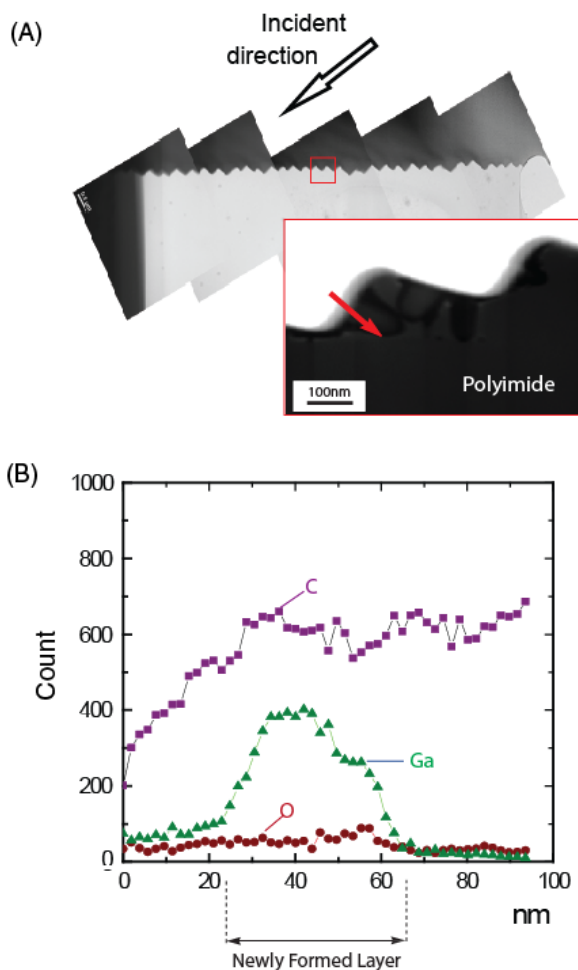
Figure 3. (A) TEM cross-sectional view of the polyimide after 5 min exposure to a FIB at the incident angle 50° (the FIB direction is from the upper right to the lower left, as shown by the white arrow). Inset: a magnified picture of the rectangular region in (A). A Pt layer was pre-deposited on the surface to protect the surface from ion beam damage during TEM sampling. The thickness of the newly formed region was periodically changed between 20 and 50 nm. The acceleration voltage and current density of the ion beam were 30 keV and 7 nA, respectively. (B) Depth profile of chemical composition of the surface layer through the direction shown by the red arrow in the magnified picture in (A) obtained using TEM EDS.

depth of the induced new surface layer was found to be non-uniform, with variations over the range 20–50 nm depending on the relative orientation of the surface with the ion beam incident angle. Figure 3(B) displays the depth profile of the distribution of key chemical components of PI (C, N, and O) measured parallel to the ion beam irradiation direction (denoted by the arrow in figure 3(A)). The newly formed layer on the PI surface has a rich Ga concentration, which is doped into the surface layer of the PI by ion beam bombardment, while the carbon concentration is relatively reduced near the surface. It is expected that the surface layer formed by the ion beam irradiation on the surface of the PI has Ga^+ doping and a semi-metallic composition, as previously shown for lower ion beam energy [27]. However, we did not carry out any experiments to examine the chemical status of the Ga (ion or

atoms) and the surface layer. The surface features may appear due to the instability of this layer, which is stiffer than the PI substrate [28, 29].

The linear relationship proposed by Bradley and Harper [2] for estimating the time evolution of the surface profile due to ion bombardment indicates that the orientation of the undulations induced by the ion beam greatly depends on the incident angle. In this theory, the energy exerted into the surface layer of the material due to Ga^+ ion bombardment is characterized by the mean penetration depth and longitudinal and lateral straggling widths. This theory, which accounts for the surface diffusion of the newly formed layer, predicts a critical incident angle for the change in the orientation of ripple morphologies by considering the diffusivity of substrate materials [2]. In our experiments, the ripple wavevector is parallel to the direction of ion beam projection for ion incident angle <55° and the amplitude of the ripples increases by increasing the irradiation time as measured in figure 2(B) for the incident angle 50°. This increase in the amplitude of the ripples leads to the formation of a step-like structure as shown in figure 1(C). However, for ion incident angles >55°, the ripple wavevector is perpendicular to the ion beam projection direction. Overall, the surface structures formed on the PI substrate due to ion beam bombardment are similar to those observed on Si substrates exposed to an ion beam [8, 11].

Figure 4 shows the application of maskless patterning of the focused ion beam system to create branching microchannels on the surface of the polymer. In figure 4(A), the incident angle is set to 0° and the exposure of the surface to the ion beam causes milling of the surface, with the milling depth depending approximately linearly on the exposure time; see figure 1(B). The same predefined pattern was used with the ion beam at an incident angle 50°; see figure 4(B). In this case, the channels are furnished with ordered ripples with wavelength ∼320 nm. Patterning the channels with nanoscale ripples can be used for particle separation [16] or to enhance mixing efficiency in microfluidics by perturbing the laminar fluidic laminar flow, as demonstrated in [30]. The acceleration voltage and current of the ion beam were 30 keV and 7 nA, respectively, in this set of experiments.

We further extended the capabilities of the above technology by using predefined patterns, which cause exposure of the polymeric surface to non-uniform ion beam intensity. Ion beam irradiation normal to the substrate surface causes milling, with a rate and depth depending on the acceleration voltage and fluence of the ion beam, respectively. Application of the maskless patterning scheme yields non-uniform ion beam irradiation of the surface and, therefore, guided creation of ordered surface structures; see figure 5. Figure 5(D) shows an example of surface structures created by the maskless pattern depicted in figure 5(A). Movie S1 (available at stacks.iop.org/Nano/20/115301) shows the evolution of the surface exposed to an ion beam with maskless patterning, which resulted in the structural feature shown in figure 5(D) after 10 min exposure to an ion beam where the acceleration voltage and current were 30 keV and 7 nA, respectively.
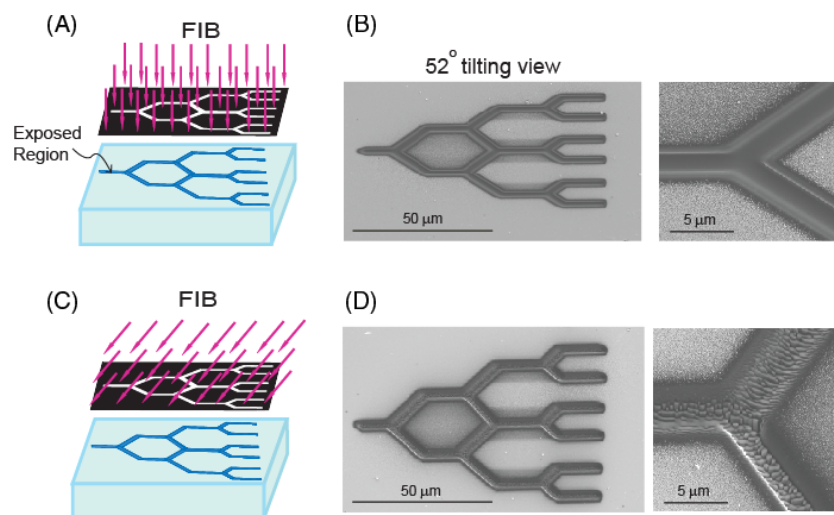
Figure 4. Branching microchannels created by the maskless patterning method. The left panels show the schematic of the experiments. The middle panels show the patterns created on the polyimide substrate, while the right panels display a magnified region of the created patterns. The ion beam incident angles were 0° and 50° in (A) and (B), respectively. The ripple structure formed in (B) has an average wavelength of ~300 nm and is comprised mainly of 1D features. In both sets of experiments, the ion beam has an acceleration voltage and a current density 30 keV and 7 nA, respectively. The total time for creation of the patterns was 3 min.
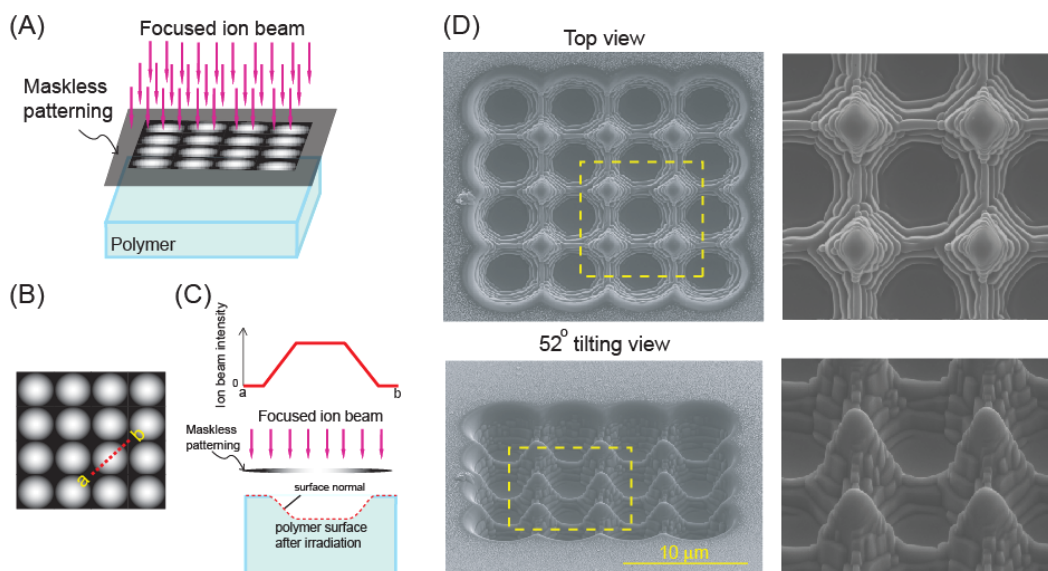
Figure 5. Maskless patterning for surface engineering of polymers. (A) Schematic of the experiment. (B) Schematic of the pattern used in the experiment. (C) Profile of the ion beam intensity in one unit cell of the pattern shown in B (along the line connecting a to b) and the schematic of the polymer surface after irradiation. Note that the ion beam is not locally normal to the surface as sculpting develops due to non-uniform surface milling. (D) Pattern created on the polyimide substrate. The ion beam has an acceleration voltage and a current density 30 keV and 7 nA, respectively. The ripple structure formed on the hills of the pattern has an average wavelength ~300 nm and is comprised of 1D and 2D features, since the local incident angle varies between 0° and ~80°. The total time for creation of this pattern was 10 min. See also movie S1 (available at stacks.iop.org/Nano/20/115301).

4. Conclusions

Nanoscale surface features on a polymeric surface were fabricated using a focused ion beam. Various patterns were identified as the incident angle was systematically varied from surface normal to almost surface parallel, yielding 1D and 2D nanoscale surface features. Moreover, the current and acceleration voltage of the focused ion beam were varied

from 1 to 20 nA and 5 to 30 keV, leading to a characteristic wavelength 80–350 nm and amplitude 10–100 nm.

Three-dimensional structures were created on the surface of the polymers by adopting the maskless patterning method of the focused ion beam system. Two different methods were introduced to control the features of the patterns at both micron and submicron scales. This includes the regions exposed to the ion beam (at the micron scale) and the morphology of

the created ripple patterns in those regions (at the submicron scale).

References

[1] Sigmund P 1973 *J. Mater. Sci.* **8** 1545
[2] Bradley R M and Harper J M 1988 *J. Vac. Sci. Technol.* A **6** 2390
[3] Li J, Stein D, McMullan C, Branton D, Aziz M J and Golovchenko J A 2001 *Nature* **412** 166
[4] Nilsson J, Lee J R I, Ratto T V and Letant S E 2006 *Adv. Mater.* **18** 427
[5] Adams D P, Vasile M J, Mayer T M and Hodges V C 2003 *J. Vac. Sci. Technol.* B **21** 2334
[6] Facsko S, Dekorsy T, Koerdt C, Trappe C, Kurz H, Vogt A and Hartnage H L 1999 *Science* **285** 1551
[7] Brown A D and Erlebacher J 2005 *Phys. Rev.* B **72** 075350
[8] Brown A D, Erlebacher J, Chan W L and Chason E 2005 *Phys. Rev. Lett.* **95** 056101
[9] Erlebacher J, Aziz M J, Chason E, Sinclair M and Floro J 1999 *Phys. Rev. Lett.* **82** 2330
[10] Cuenat A, George H B, Chang K C, Blakely J and Aziz M J 2005 *Adv. Mater.* **17** 2845
[11] Ziberi B, Frost F, Rauschenbach B and Hoche T 2005 *Appl. Phys. Lett.* **87** 033113
[12] Ziberi B, Frost F and Rauschenbach B 2006 *Appl. Phys. Lett.* **88** 173115
[13] Moon M-W, Lee S H, Sun J-Y, Oh K H, Vaziri A and Hutchinson J W 2007 *Proc. Natl Acad. Sci. USA* **104** 1130
[14] Moon M-W, Lee S H, Sun J-Y, Oh K H, Vaziri A and Hutchinson J W 2007 *Scr. Mater.* **57** 747
[15] Moon M-W, Her E K, Oh K H, Lee K R and Vaziri A 2008 *Surf. Coat. Technol.* **202** 5319
[16] Efimenko K, Rackaitis M, Manias E, Vaziri A, Mahadevan L and Genzer J 2005 *Nat. Mater.* **4** 293
[17] Loh O, Vaziri A and Espinosa H D 2009 *Exp. Mech.* **49** 105–24
[18] Chan E P and Crosby A J 2006 *Adv. Mater.* **18** 3238
[19] Wilder E A, Guo S, Lin-Gibson S, Fasolka M J and Stafford C M 2006 *Macromolecules* **39** 4138
[20] Ghosh M K and Mittal K L 1996 *Polyamides: Fundamentals and Applications* (New York: Dekker)
[21] Ali M, Schiedt B, Healy K, Neumann R and Ensinger W 2008 *Nanotechnology* **19** 085713
[22] Metz S, Bertsch A, Bertrand D and Renaud P H 2004 *Biosens. Bioelectron.* **19** 1309
[23] Kawakami H, Hiraka K, Nagaoka S, Suzuki Y and Iwaki M 2004 *J. Artif. Organs* **7** 83
[24] Richardson R R Jr, Miller J A and Reichert W M 1993 *Biomaterials* **14** 627
[25] Feili D, Schuettler M, Doerge T, Kammer S, Hoffmann K P and Stieglitz T 2006 *J. Micromech. Microeng.* **16** 1555
[26] Mishra P and Ghose D 2006 *Phys. Rev.* B **74** 155427
[27] Lazareva I, Koval Y, Alam M, Strömsdörfer S and Müller P 2007 *Appl. Phys. Lett.* **90** 262108
[28] Dong H and Bell T 1999 *Surf. Coat. Technol.* **111** 29
[29] Hozumi A, Masuda T, Sugimura H and Kameyama T 2003 *Langmuir* **19** 7573
[30] Stone H A, Stroock A D and Ajdari A 2004 *Annu. Rev. Fluid Mech.* **36** 381